NJC

PAPER

View Article Online
View Journal

Cite this: DOI: 10.1039/c9nj01787a

Self-assembly with fluorescence readout in a free base dipyrrin–polymer triggered by metal ion binding in aqueous solution†

Rui Liu, Pothiappan Vairaprakash and Jonathan S. Lindsey *

A hydrophobic dipyrrin has been attached to a heterotelechelic amphiphilic random copolymer as part of a single-polymer–single-cargo strategy. The polymer–dipyrrin ("**Pod-dipyrrin**") exhibits an extended conformation in the organic solvent *N*,*N*-dimethylformamide (DMF) but in aqueous solution forms a unimeric nanoparticle (*i.e.*, a foldamer) as indicated by dynamic light-scattering (DLS) data (hydrodynamic diameter D_h = 140 nm *versus* 15 nm in the two solvents, respectively). Treatment of the **Pod-dipyrrin** with Zn(II) in aqueous solution causes formation of a bis(Pod-dipyrrinato)Zn(II) complex as evidenced by a (1) slight change in absorption spectrum, (2) ~50-fold increase in fluorescence quantum yield (Φ_f from 0.0035 to 0.17), and (3) profound increase in D_h (from 15 nm to 260 nm). The D_h value for the bis(Pod-dipyrrinato)Zn(II) complex is only slightly smaller in water (260 nm) than in DMF (310 nm), where a more extended conformation is expected. The increase in fluorescence of the bis(Pod-dipyrrinato)Zn(II) complex is readily observed by visual inspection (*i.e.*, naked-eye readout). The conversion of a compact folded unimer (15 nm) to a more extended dimer (260 nm) triggered by metal ion addition denotes a conformationally malleable, environmentally sensitive molecular architecture. The self-assembly process can be reversed upon treatment with a metal-ion sequestering agent such as EDTA. The facile synthesis of a fluorogenic architecture that undergoes profound spontaneous change in molecular morphology upon binding an exogenous agent in water under physiological conditions may open a number of opportunities for sensory-mechanical studies in the life sciences.

Received 8th April 2019,
Accepted 13th May 2019

DOI: 10.1039/c9nj01787a

rsc.li/njc

Introduction

The absorption and fluorescence spectra of organic chromophores make for diverse applications in the life sciences yet the tailoring of chromophores for solubility in aqueous media often presents significant challenges. Absorption and fluorescence in the visible region inevitably entail a sizeable π-chromophore, at least for intense π–π* transitions. The vast majority of dyes contain a chromophore that bears intrinsic charge,[1] which also facilitates solubilization in aqueous media. For chromophores that lack intrinsic charge (*e.g.*, carotenoids, perylenes, quinones, tetrapyrroles),[1] the challenge of aqueous solubilization is acute. While solubilizing substituents can often be incorporated, in many cases the size of the π-system requires construction of a daunting superstructure to impart adequate aqueous solubility.

We recently reported a new and simpler approach for aqueous solubilization of neutral or moderately polar chromophores.[2] The approach – extending extensive work by the groups of Sawamoto[3,4] and Zimmerman[5,6] – entails covalent attachment of the chromophore to one terminus of an amphiphilic random copolymer, thereby affording a single-polymer–single-chromophore construct. The polymer "folds" around the unadorned chromophore and enables the resulting "pod-chromophore" to dissolve in aqueous solution. This approach separates the chromophore design and aqueous solubilization into two separate spheres – chromophore cargo and polymer package – with covalent joining of the two entities in the final synthetic step. To date, the polymer that we have employed (**F-Ph**)[2] is a polyacrylate/polyacrylamide containing three types of pendant groups and distinct functional groups at the two backbone termini (*i.e.*, heterotelechelic). The three types of pendant groups: a methoxy-terminated oligoethylene glycol (PEG9; polar but nonionic), a sulfonate-terminated short alkyl chain (ionic), and a lauryl (hydrophobic) group are incorporated from three corresponding monomers *via* living radical polymerization. The chain-transfer agent in the polymerization ultimately provides the two terminal functional groups, which

Department of Chemistry, North Carolina State University, Raleigh, North Carolina 27695-8204, USA. E-mail: jlindsey@ncsu.edu

† Electronic supplementary information (ESI) available: Results upon complexation of **Pod-Dipyrrin** with various ZnX_2; and NMR spectra for all new compounds. See DOI: 10.1039/c9nj01787a

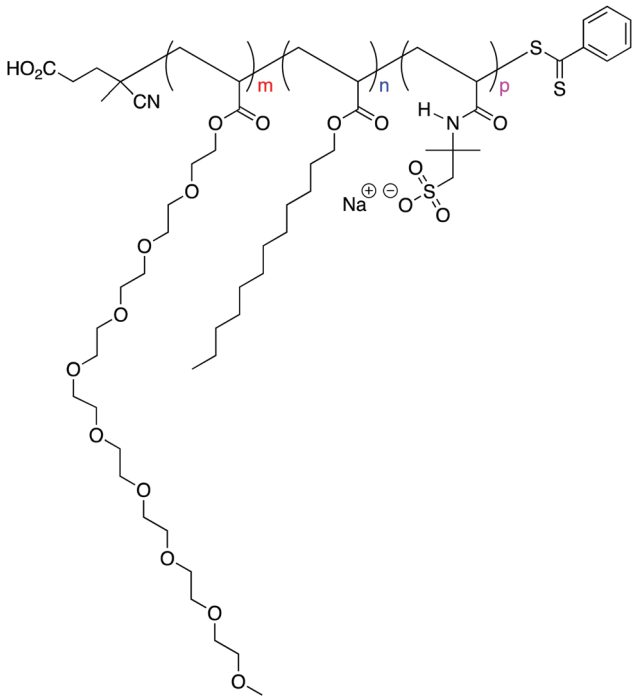

Chart 1 General design of the heterotelechelic amphiphilic random copolymer for encapsulation of a covalently attached hydrophobic fluorophore in aqueous solution. For **F-Ph**, $m:n:p$ = 1 : 1 : 5 ratio with overall molecular weight of 40 kDa (m, $n \sim 20$ and $p \sim 100$).

in this case are carboxylic acid and dithiobenzoate groups (Chart 1). The success relied on identification of the appropriate ratios of the three monomers ($m:n:p$ = 1 : 1 : 5 ratio of PEG9, lauryl and sulfonate-terminated units), affording polymer **F-Ph**[2] of size 40 kDa where m, $n \sim 20$ and $p \sim 100$.

This foldamer approach proved viable with 8 classes of chromophores including those that are neutral and hydrophobic (bacteriochlorin, BODIPY, chlorin, coumarin, perylene, phthalocyanine) or intrinsically charged (cyanine, rhodamine).[2] The presence of one and only one chromophore per pod resulted in absorption and fluorescence features of the pod-chromophore in aqueous solution that were essentially identical to those of the hydrophobic chromophore in an organic solvent (*e.g.*, toluene; *N*,*N*-dimethylformamide, DMF). In addition, the fluorescence quantum yield (Φ_f) was little changed for the pod-chromophore in water *versus* the chromophore alone in organic media, thus exhibiting none of the insidious diminution of fluorescence brightness[7] so often encountered upon placing an organic chromophore in aqueous media.

One objective in developing the single-polymer–single-chromophore foldamer approach was to embed the chromophore in the inner confines of the polymer, insulated from the surrounding environment. One chromophore examined was a fluorogenic rhodamine–lactam that upon exposure to metal ions is known to undergo ring-opening, thereby eliciting fluorescence. Upon treatment of the **Pod-Rhodamine** with various metal ions, the fluorescence turn-on phenomenon was observed.[2] This result implies that the fluorophore is not irrevocably incarcerated in the inner space of the folded polymer but does have exposure, or at least excursions, to the outside milieu.

Here, we report our results concerning the metal binding of a single dipyrrin in the polymer. We first describe the synthesis of a maleimide-containing free base dipyrrin, then attach the dipyrrin to the thiol group in the heterotelechelic amphiphilic random copolymer described above. The resulting single-polymer–single-dipyrrin architecture (**Pod-Dipyrrin**) was examined for binding of divalent zinc and copper ions. The formation of the bis(dipyrrinato)metal(II) complex would entail intermolecular interaction of two pods rather than interaction with a single pod as in the **Pod-Rhodamine** study. The fluorogenic response here also is completely distinct from the common process where amine-based photoinduced electron transfer is suppressed upon metal binding, thereby turning on fluorescence. The studies have led to new insights concerning fluorescence of the free base dipyrrin, intrinsic properties of the pod architecture, and morphological changes of the polymer–dipyrrin entity upon binding metal ions.

Results and discussion

1. Dipyrrin molecular design

Free base dipyrrins bearing diverse substituents react readily with various metal ions (such as Zn^{2+}, Mg^{2+}, Ni^{2+}, Co^{2+}, Cu^{2+}, Pd^{2+}, In^{3+}, Ga^{3+}, *etc.*) to form the corresponding bis(dipyrrinato)metal(II) (or tris(dipyrrinato)metal(III)) complexes. The bis(dipyrrinato)metal(II) complexes absorb strongly in the blue-green region ($\varepsilon \sim 50\,000$–$100\,000\ M^{-1}\ cm^{-1}$). Although first reported by Fischer in 1924,[8] the complexes were long considered to be non-fluorescent and were little investigated.[9] Replacement of the phenyl group at the dipyrrin 5-position with the sterically encumbering mesityl group increased the fluorescence quantum yield of the corresponding bis(dipyrrinato)Zn(II) complexes by a factor of 60, from Φ_f = 0.006 of the 5,5′-phenyl substituted complex **I** to 0.36 of the 5,5′-mesityl substituted complex **II** (Chart 2).[10] The very large increase in fluorescence intensity makes the resulting complexes viable for use as legitimate fluorescent dyes. Accordingly, for the

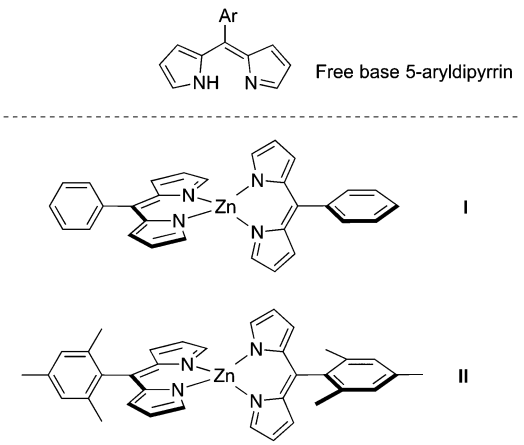

Chart 2 Free base dipyrrin and two bis(dipyrrinato)Zn(II) complexes.

free base dipyrrin here, we chose an analogous system wherein the 5-aryl group is equipped with 2,6-dimethyl groups and a tether at the 4-position. The presence of an amino or alkoxy group at the *p*-position of the 5-phenyl group is known to cause quenching of the BODIPY analogues[11] (presumably *via* internal charge transfer), hence we chose to join the tether to the aryl *p*-position *via* a carbonyl group.

2. Synthesis of the bioconjugatable dipyrrin

The known aryl aldehyde 4-iodo-2,6-dimethylbenzaldehyde (**1**)[12,13] was dissolved in pyrrole (serving as reactant in excess and solvent) and treated with trifluoroacetic acid at room temperature in a one-flask synthesis[14,15] (Scheme 1). The corresponding dipyrromethane **2** was obtained in 60% yield without aqueous/organic extraction. The aminocarbonylation of **2** with *N*-(*tert*-butoxycarbonyl)-1,6-diaminohexane was attempted using $Mo(CO)_6$ as a solid source of carbon monoxide,[16–20] but the mono- and di-carbonylated products were obtained in yields of 11% and 10%, respectively. Upon use of $Pd(OAc)_2$/Xantphos/Cs_2CO_3 in an atmosphere of CO,[21,22] the desired product dipyrromethane **3** was obtained in 61% yield. Treatment of **3** with *p*-chloranil in THF at room temperature for 24 h afforded **4** in 69% yield. The oxidation could be completed within 1 h by sonicating the reaction mixture instead of stirring at room temperature for 24 h. The removal of the *tert*-butoxycarbonyl group of **4** and introduction of the maleimido moiety were carried out in a single flask process. Thus, treatment of **4** with trifluoroacetic acid in CH_2Cl_2 for 12 h caused removal of the *tert*-butoxycarbonyl group as confirmed by TLC analysis. The resulting residue after the removal of the volatile substances was treated with 6-maleimidohexanoic acid and *O*-(benzotriazol-1-yl)-*N*,*N*,*N*′,*N*′-tetramethyluronium hexafluorophosphate (HBTU) in CH_2Cl_2 containing *N*,*N*-diisopropylethylamine (DIEA) for 2 h. Workup and chromatography afforded dipyrrin **5** in 77% yield. Finally, treatment

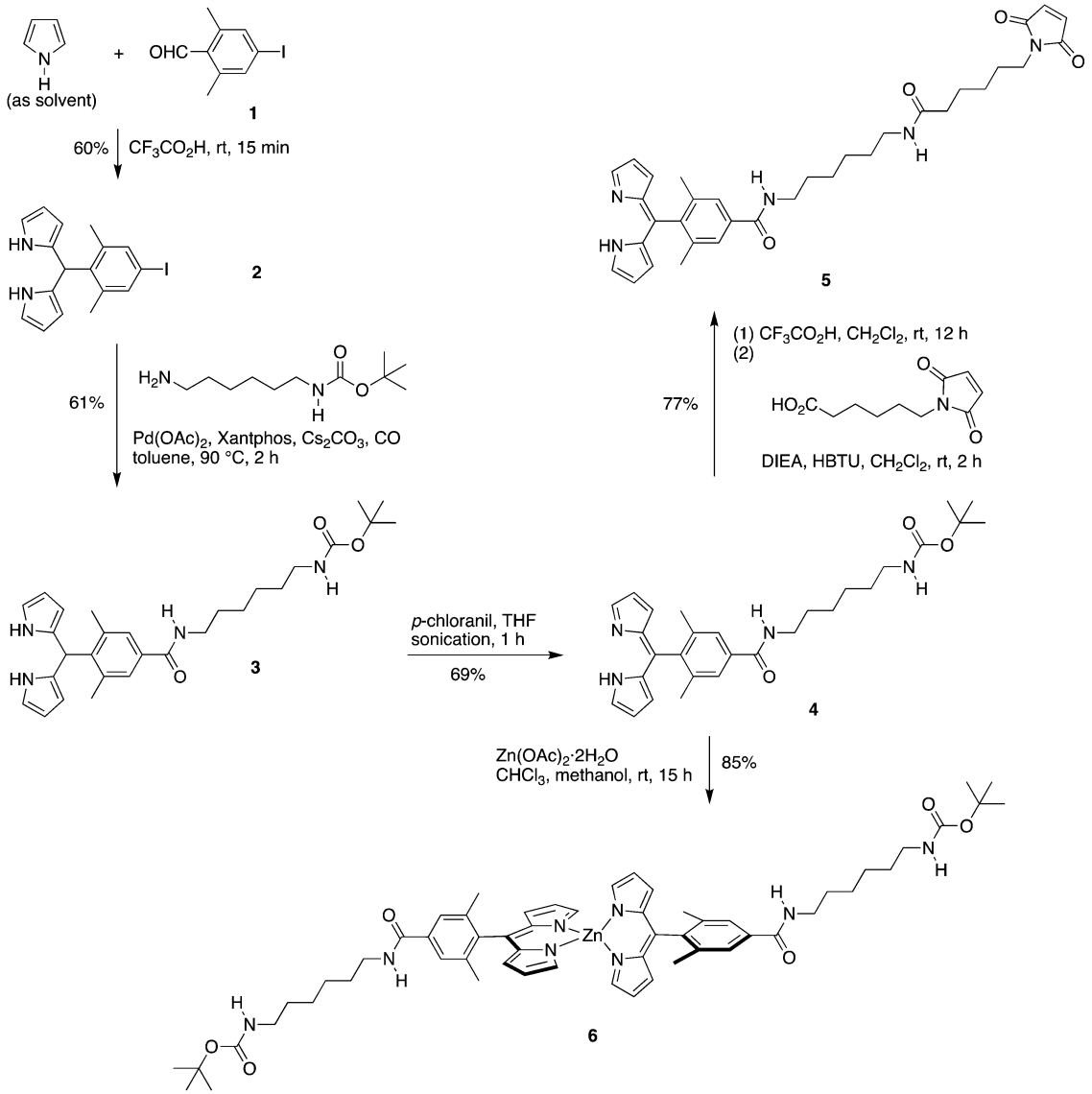

Scheme 1 Synthesis of dipyrromethanes **2** and **3**; dipyrrins **4** and **5**; and bis(dipyrrinato)Zn(II) complex **6**.

of the dipyrrin **4** with zinc acetate afforded bis(dipyrrinato)Zn(II) complex **6**. Each new compound was characterized by ^{1}H NMR and ^{13}C NMR spectroscopy as well as accurate mass determination by electrospray ionization mass spectrometry (ESI-MS). The ^{1}H NMR spectrum of the free base dipyrrins (**4**, **5**) showed peaks due to all protons, with the exception of that of the pyrrole N–H in the dipyrrin moiety. This feature has been encountered previously with other free base dipyrrins.[9]

The absorption and fluorescence properties of the bis(dipyrrinato)Zn(II) complex **6** were examined in toluene (Fig. 1). Coordination complex **6** has sharp absorption (fwhm 35 nm) and fluorescence (fwhm 32 nm) bands compared to those of free base dipyrrin **4** in toluene. The bis(dipyrrinato)Zn(II) complex **6** exhibits Φ_f = 0.16, to be compared with 0.0011 of the free base dipyrrin **4**. For these and all subsequent measurements, the fluorescence standard is a BODIPY-hydrazide (Φ_f = 0.97).[2] Self-assembly of the two free base dipyrrins into a bis(dipyrrinato)Zn(II) complex equipped with 2,6-dimethylaryl moieties affords a substantially brighter chromophore. The fluorescence spectra of matched samples of **6** and **II** in toluene were found to be essentially identical, although the Φ_f value of **6** (0.18) was exactly half that of **II** (0.36)[10] using **II** as the standard. The complexes differ only in the nature of the *p*-aryl substituent (amido *versus* methyl); hence the amido substituent apparently causes diminution of the fluorescence intensity.

The absorption and fluorescence spectral properties of the bis(dipyrrinato)Zn(II) complex **6** also were examined in organic solvents of a range of polarity. The solvents range from the nonpolar toluene to the quite polar DMF. The spectra are displayed in Fig. 2. The absorption maximum varies little (from 482–488 nm) although slightly greater variation occurs in the position of the fluorescence maximum (493–503 nm), giving a Stokes shift range of 9–15 nm (Table 1). The Φ_f values decline with increasing polarity, from Φ_f = 0.18 in toluene to 0.041 in DMF, although the spectra shapes are little changed with solvent polarity.

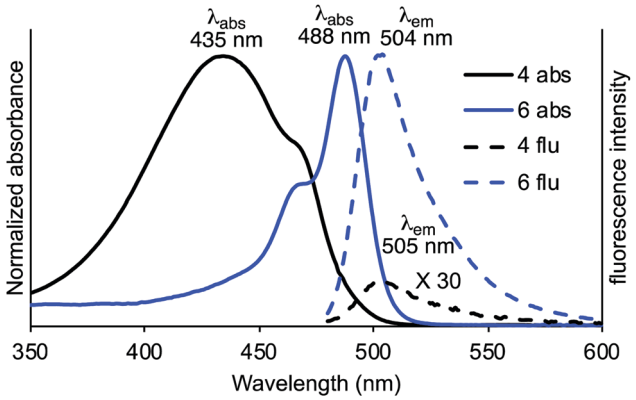

Fig. 1 Electronic spectra in toluene at room temperature. Absorption (blue solid line, λ_{max} = 488 nm) and fluorescence (λ_{exc} 460 nm, blue dashed line, λ_{max} = 504 nm) of bis(dipyrrinato)Zn(II) complex **6**, and absorption (black solid line, λ_{max} = 435 nm) and fluorescence (λ_{exc} 390 nm, black dashed line, λ_{max} = 505 nm) of free base dipyrrin **4**.

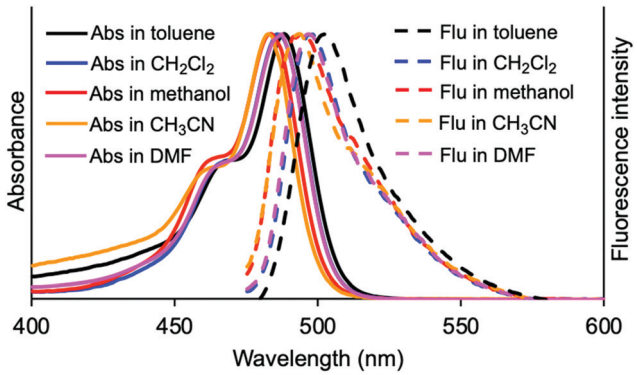

Fig. 2 Absorption and fluorescence spectra (normalized) of **6** in toluene (black line), dichloromethane (blue line), methanol (red line), acetonitrile (orange line), and DMF (magenta line).

Table 1 Spectral properties of **6** in organic solvents

Entry	Solvent	Dielectric constant	λ_{abs} (nm)	λ_{em} (nm)	Stokes shift (nm)	fwhm λ_{em} (nm)	Φ_f[a]
1	Toluene	2.4	488	503	15	30	0.18
2	CH_2Cl_2	9.1	486	498	12	27	0.079
3	Methanol	32.6	485	494	9	35	0.032
4	Acetonitrile	36.6	482	493	11	34	0.050
5	DMF	38.3	487	496	9	27	0.041

[a] All yield data were obtained with compound **II** as a reference (Φ_f = 0.36).[10]

3. Synthesis of the polymer–dipyrrin conjugate

Synthesis of **Pod-Dipyrrin** follows the procedure employed previously[2] (Scheme 2). Treatment of polymer **F-Ph** in DMF containing triethylamine and ethanolamine liberated the free thiol, which was reacted *in situ* with dipyrrin-maleimide **5**. The crude reaction mixture in DMF was dialyzed to remove any free fluorophore, which has been readily achieved previously with diverse chromophores.[2] The conjugation and purification process required ~4 days, whereupon **Pod-Dipyrrin** was obtained as a yellow friable powder.

4. Characterization of the Pod-Dipyrrin

The **Pod-Dipyrrin** was examined by ^{1}H NMR spectroscopy in D_2O at room temperature. Characteristic peaks were observed for the polymer constituents but not of the dipyrrin moiety, which is not surprising given that the latter is present on one terminus of the polymer and represents only ~1.5% of the mass of the construct. While the extent of conjugation cannot be readily established by NMR analysis, evidence presented below supports the interpretation that the conjugation has gone to completion. We turned to studies of the photophysical properties of **Pod-Dipyrrin** in water. The absorption spectrum of **Pod-Dipyrrin** (Fig. 3A, black solid line) in aqueous solution shows a narrower absorption peak (full-width-at-half-maximum, fwhm 39 nm) compared to that of the hydrophobic benchmark **5** (fwhm 80 nm) in toluene (Fig. 3B, red solid line). The narrower absorption feature may stem from restricted conformational motion of the dipyrrin unit in **Pod-Dipyrrin**

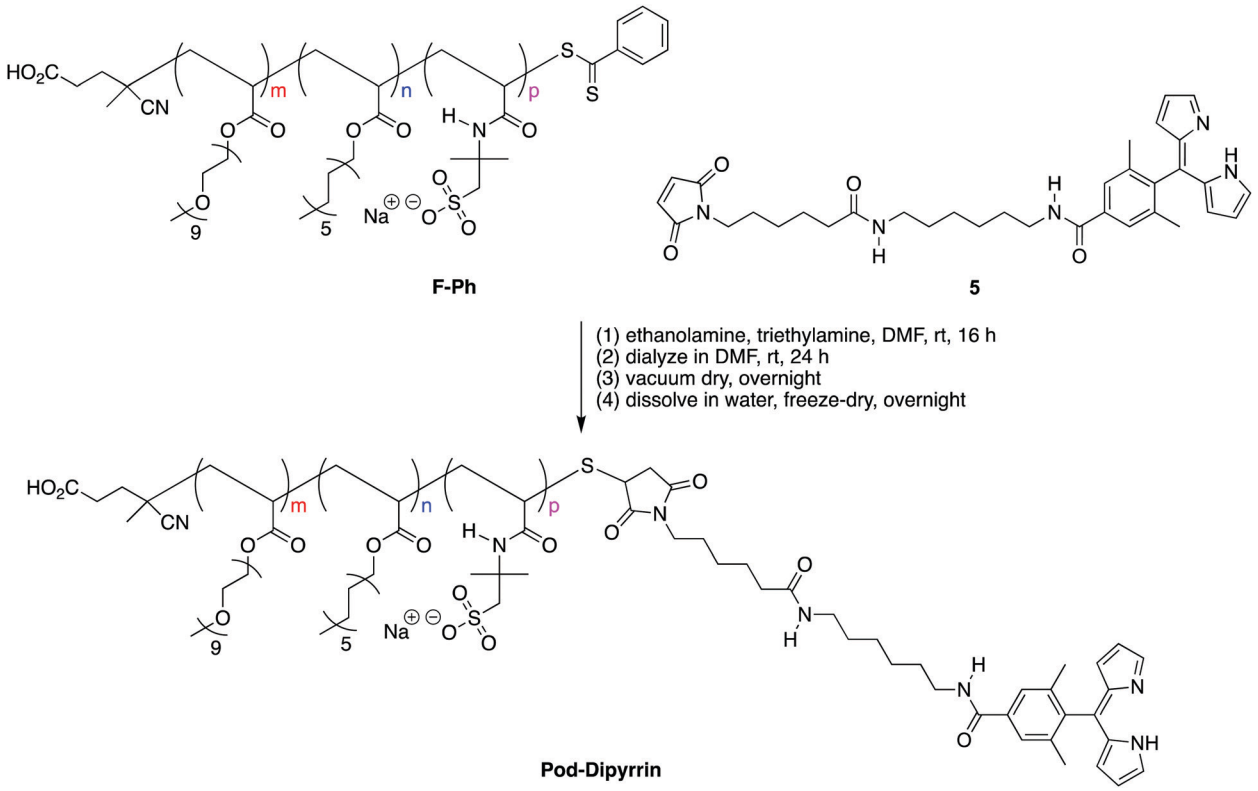

Scheme 2 Synthesis of **Pod-Dipyrrin**.

due to the folded state of the amphiphilic polymer in aqueous solution, whereas the dipyrrin chromophore of hydrophobic benchmark **5** has a fuller range of motion in toluene. The motions include butterfly flexing[10,23] of the dihedral planes of the pyrroles with respect to each other, and the rotation of the aryl group about its *p*-substituted axis. **Pod-Dipyrrin** in water has a weak and broad fluorescence peak similar to that of **5** in toluene.

The **Pod-Dipyrrin** was examined by dynamic light-scattering (DLS) spectroscopy in aqueous solution at concentrations ranging from 10–1 mg mL^{-1}, the approximate lower limit of the DLS instrument. Essentially identical size distributions were observed over this concentration range indicating the integrity of the folded architecture (Fig. 4A). On the other hand, the **Pod-Dipyrrin** showed a profound difference in molecular size in DMF *versus* water (Fig. 4B). In DMF the size distribution is peaked at a hydrodynamic diameter D_h = 140 nm, whereas the distribution peak is 15 nm in water. The results are consistent with folding to form a compact unimer in aqueous solution from a more extended and unstructured set of conformations in the organic solvent DMF. The absorption spectrum of **Pod-Dipyrrin** (Fig. 4C) also is much narrower in water (fwhm 39 nm) than in DMF (fwhm 79 nm). These absorption spectral changes are similar to those for **Pod-Dipyrrin** in water *versus* **5** in toluene (Fig. 3B). The data are fully consistent with expectations concerning folding in aqueous solution on the basis of prior data of the same polymer bearing other families of chromophores.[2]

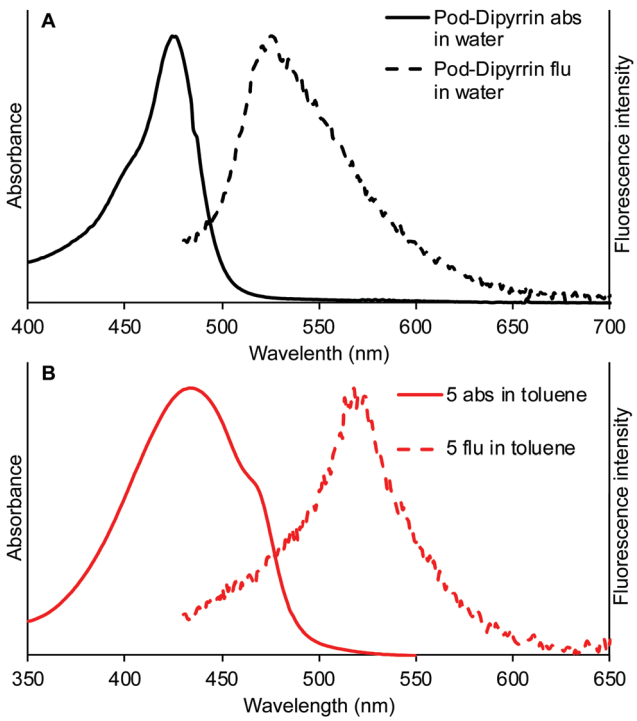

Fig. 3 (A) Absorption (solid line) and fluorescence (λ_{exc} 460 nm, dashed line) spectra of **Pod-Dipyrrin** in water; and (B) absorption (red solid line) and fluorescence (λ_{exc} 390 nm, red dashed line) spectra of free base dipyrrin **5** in toluene.

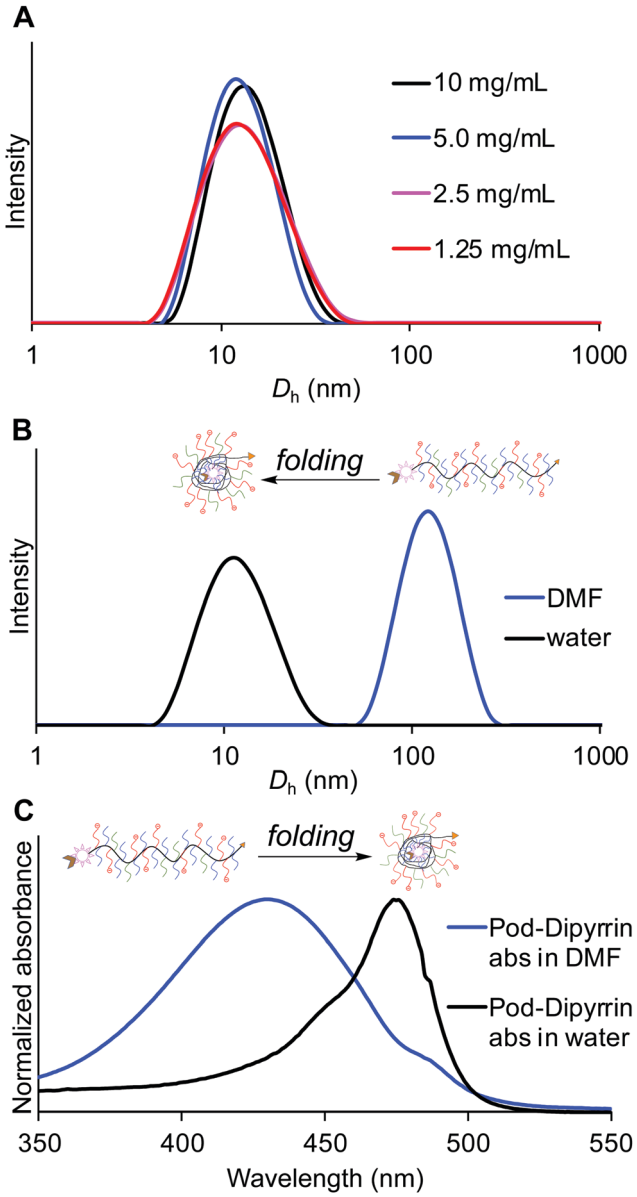

Fig. 4 Properties of **Pod-Dipyrrin** at room temperature. (A) DLS data in 1 M aqueous NaCl at various concentrations: (A) 10 mg mL^{-1}, average diameter 14.8 nm; 5.0 mg mL^{-1}, 13.4 nm; 2.5 mg mL^{-1}, 14.8 nm; and 1.25 mg mL^{-1}, 14.5 nm. (B) DLS data in DMF (blue line) and water (black line) at 1.0 mg mL^{-1}, and (C) absorption in DMF (blue line) and water (black line) at 1.0 mg mL^{-1}.

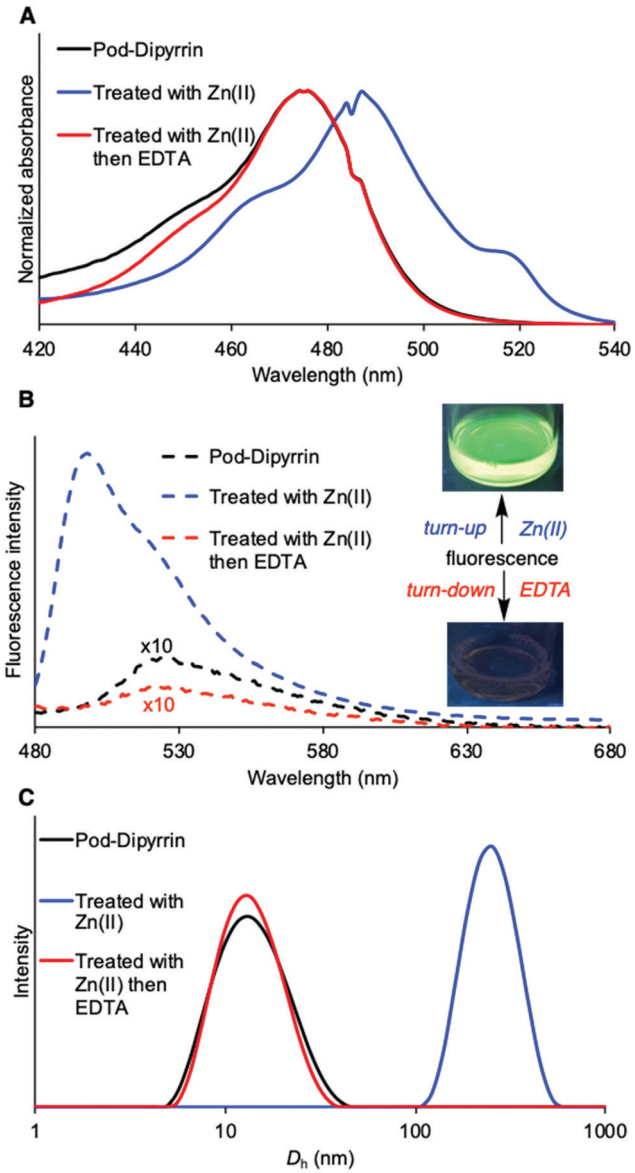

Fig. 5 Spectral and DLS data in water at room temperature. (A) Absorption spectra of **Pod-Dipyrrin** at 1 mg mL^{-1} (black line), **Pod-Dipyrrin** treated with Zn(II) (blue line), and **Pod-Dipyrrin** treated with Zn(II) then EDTA (red line); (B) fluorescence spectra of **Pod-Dipyrrin** (black dashed line), **Pod-Dipyrrin** treated with Zn(II) (blue dashed line), and **Pod-Dipyrrin** treated with Zn(II) then EDTA (red dashed line); (C) DLS data of **Pod-Dipyrrin** at 1 mg mL^{-1} (black line), **Pod-Dipyrrin** treated with Zn(II) (blue line), and **Pod-Dipyrrin** treated with Zn(II) then EDTA (red line). In all treatments, Zn(II) refers to $Zn(OAc)_2$ (440 equiv.).

5. Self-assembly of the Pod-Dipyrrin *via* metal ion chelation in water

We have demonstrated that a related polymer–fluorophore is able to bind metals in aqueous solution.[2] Here, we tested the ability of **Pod-Dipyrrin** to form dimeric pod assemblies owing to formation of the di(pyrrinato)metal(II) complexes upon the introduction of divalent metal ions (Zn(II) and Cu(II)). A solution of **Pod-Dipyrrin** in aqueous solution was treated with excess $Zn(OAc)_2$ (440 equiv.) at room temperature. Examination by absorption spectroscopy after 5 minutes revealed a bathochromic shift (12 nm) compared to the monomeric **Pod-Dipyrrin** in water (Fig. 5A). The fluorescence quantum yield (Φ_f = 0.17) also increased profoundly (~50-fold) compared to that of **Pod-Dipyrrin** (Φ_f = 0.0035 in water) (Fig. 5B). Such changes in absorption and fluorescence are attributed to the formation of the bis(dipyrrinato)Zn(II) complex, which must then join two pod architectures; the resulting assembly is termed **(Pod-Dipyrrin)$_2$Zn(II)**. The aforementioned spectral changes are visibly evident: (1) the free base dipyrrin in solution is yellow whereas the bis(dipyrrinato)Zn(II) complex is light yellow; and (2) upon illumination, no fluorescence

Table 2 Photophysical properties of diverse constructs in organic or aqueous media

Entry	Compound	Solvent	λ_{abs} (nm)	λ_{exc} (nm)	λ_{em} (nm)	fwhm λ_{em} (nm)	Φ_f[a]
1	**4**	Toluene	435	390	505	34	0.0011
2	**5**	Toluene	434	390	518	54	0.0006
3	**6**	Toluene	488	460	504	32	0.16
4	**Pod-Dipyrrin**	Water	474	460	526	61	0.0035
5	**Pod-Dipyrrin**	DMF	430	390	530	80	0.0021
6	**(Pod-Dipyrrin)$_2$Zn(II)**	DMF	486	460	496	27	0.11
7	**(Pod-Dipyrrin)$_2$Zn(II)**	Water	487	470	498	43	0.17

[a] All yield data obtained with **BDPY-hydrazide** as a reference (Φ_f = 0.97).[2,24]

is visible from the free base dipyrrin whereas the bis(dipyrrinato)Zn(II) complex exhibits a green glow. The fluorescence properties of the **Pod-Dipyrrin** species in water are shown in Table 2 and can be compared with those of **Pod-Dipyrrin** (in DMF) and **5** in toluene. The spectral properties of the **(Pod-Dipyrrin)$_2$Zn(II)** are described further in the Discussion section.

The free base **Pod-Dipyrrin** and the assembled **(Pod-Dipyrrin)$_2$Zn(II)** were examined by DLS spectroscopy. The free base **Pod-Dipyrrin** is unimeric in water with a peak in the DLS distribution at 15 nm (Fig. 5C). On the other hand, the **(Pod-Dipyrrin)$_2$Zn(II)** exhibits large very assemblies of 260 nm in dimension; such large assemblies are unexpected because the simplest architecture would be simply twice the size of a single **Pod-Dipyrrin**. The data imply the **(Pod-Dipyrrin)$_2$Zn(II)** must unfold upon formation of the bis(dipyrrinato)Zn(II) motif.

Upon treatment of the **(Pod-Dipyrrin)$_2$Zn(II)** assembly in aqueous solution with excess EDTA (3.2 equiv. per the total quantity of Zn(II)), several distinct changes occurred: (1) the absorption features reverted to those of the unimeric free base **Pod-Dipyrrin** (Fig. 5A), reflecting a change in color from light green to yellow; (2) the fluorescence diminished markedly and visibly, to a slightly lower level than for the **Pod-Dipyrrin** alone (Fig. 5B); and (3) DLS data revealed the reversion from the large assembly to give the unimeric folded architecture characteristic of **Pod-Dipyrrin** (Fig. 5C). The combined evidence of absorption shifts, fluorescence brightness and size changes reveal a reversible conversion of **Pod-Dipyrrin** to **(Pod-Dipyrrin)$_2$Zn(II)** in water accompanied by a profound mechanical change and fluorescence readout: fluorescence turn-up upon addition of Zn(II) and turn-down upon removal of Zn(II).

The self-assembly experiment with **Pod-Dipyrrin** was also carried out with Cu(II) in water. Upon treatment with 600 equiv. of $CuCl_2$, the absorption spectrum shows a bathochromic shift (17 nm) (Fig. 6A), the fluorescence was strongly quenched (Fig. 6B), and the DLS data showed conversion of the compact unimer (D_h = 15 nm) to a large assembly (D_h = 230 nm) (Fig. 6C), all of which signal the formation of **(Pod-Dipyrrin)$_2$Cu(II)**. Treatment with excess EDTA (2.3 equiv. per the total quantity of Cu(II)) caused reversion to the absorption spectrum and unimeric size of the **Pod-Dipyrrin**. The fluorescence increases but only slightly, without full recovery of the fluorescence expected of the **Pod-Dipyrrin**; one interpretation is that the copper–EDTA complex (green) is associated with the **Pod-Dipyrrin** and causes quenching of the free base dipyrrin. The combined evidence of absorption, fluorescence brightness and size changes reveal a reversible self-assembly of **Pod-Dipyrrin** in water with fluorescence turn-off upon addition of Cu(II) and turn-on upon removal of Cu(II).

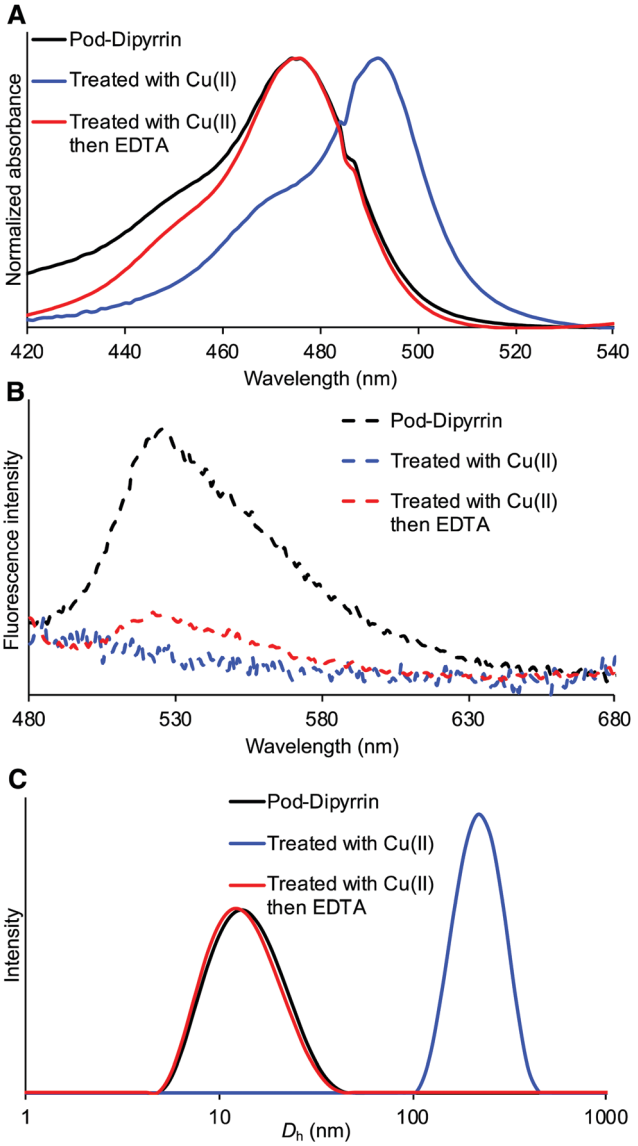

Fig. 6 All data were collected in water at room temperature. (A) Absorption spectra of **Pod-Dipyrrin** at 1 mg mL^{-1} (black solid line), **Pod-Dipyrrin** treated with Cu(II) (red solid line), and **Pod-Dipyrrin** treated with Cu(II) then EDTA (red solid line); (B) fluorescence spectra of **Pod-Dipyrrin** (black dashed line), **Pod-Dipyrrin** treated with Cu(II) (red dashed line), and **Pod-Dipyrrin** treated with Cu(II) then EDTA (red dashed line); (C) DLS data of **Pod-Dipyrrin** at 1 mg mL^{-1} (black solid line), **Pod-Dipyrrin** treated with Cu(II) (red solid line), and **Pod-Dipyrrin** treated with Cu(II) then EDTA (red solid line). In all treatments, Cu(II) refers to $CuCl_2$ (600 equiv.).

The observed size distribution of **(Pod-Dipyrrin)$_2$Zn(II)** (260 nm) in water matches that of two unfolded **F-Ph** (130 nm × 2) polymers in DMF, but is far larger than expected for the simple dimerization of two intact unimers (15 nm × 2) in water. To explore such large

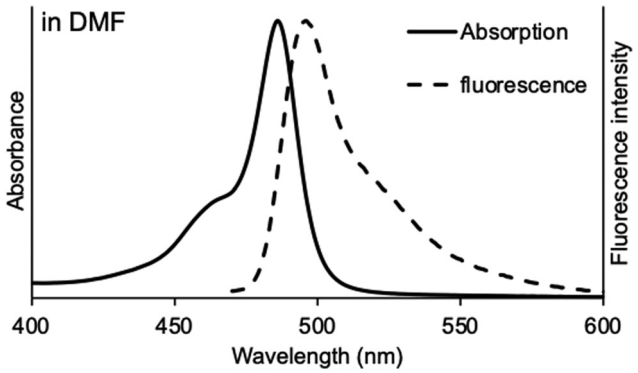

Fig. 7 Absorption (solid line) and fluorescence (dashed line) spectra of **(Pod-Dipyrrin)$_2$Zn(II)** in DMF at room temperature.

size distributions, the assembly of **Pod-Dipyrrin** was carried out in DMF. Treatment of **Pod-Dipyrrin** in DMF with $Zn(OAc)_2$ resulted in formation of the corresponding **(Pod-Dipyrrin)$_2$Zn(II)** as seen by the absorption spectrum (Fig. 7). Examination by DLS spectroscopy shows that the free base **Pod-Dipyrrin** in DMF exhibits D_h = 140 nm (Fig. 8A) whereas the **(Pod-Dipyrrin)$_2$Zn(II)** exhibits a much larger D_h = 310 nm (Fig. 8B). Finally, treatment of polymer **F-Ph** with $Zn(OAc)_2$ in water resulted in no noticeable size change (Fig. 8C), as expected for a polymer that lacks a dipyrrin unit altogether.

To probe the self-assembly process, **Pod-Dipyrrin** in aqueous solution was titrated with zinc acetate. The addition of 1 equiv. gave two peaks upon DLS spectroscopic examination, including that of the uncomplexed unimer (D_h = 13 nm) and that for the putative dimer at D_h = 200 nm (Fig. 9). Treatment with 10 equiv. caused loss of the unimer peak and only the putative dimer peak was observed. No further change was observed with 100 equiv. In this titration, no peaks intermediate between that of unimer and dimer were observed.

Discussion

The development of foldamers enables diverse molecular entities to be packaged in a relatively hydrophobic enclosure for use in aqueous solution. The distinct feature of the strategy we are developing enables packaging of a single item of molecular cargo per polymer chain. The idea behind individual packaging of a single molecular item was developed to preclude quenching of fluorophores and deleterious contact with water while achieving use in water. A limiting view is that the fluorophore or other hydrophobic cargo item is ensconced in the interior of the self-assembled foldamer. Yet the results herein show that the cargo item – the dipyrrin – can bind with metal ions in aqueous solution, and in so doing cause substantial structural change of the foldamer package. Hence the foldamer is not like a rigid marble but is highly malleable and poised for morphological alteration. In the following sections, we first discuss the spectra and photophysics of dipyrrins. We then discuss experiments that bear on the environmental polarity of the polymer-bound bis(dipyrrinato)Zn(II) complex. We finish by considering the mechanical change associated with the self-assembly process leading to the bis(dipyrrinato)-metal complexes from the foldamer–dipyrrin.

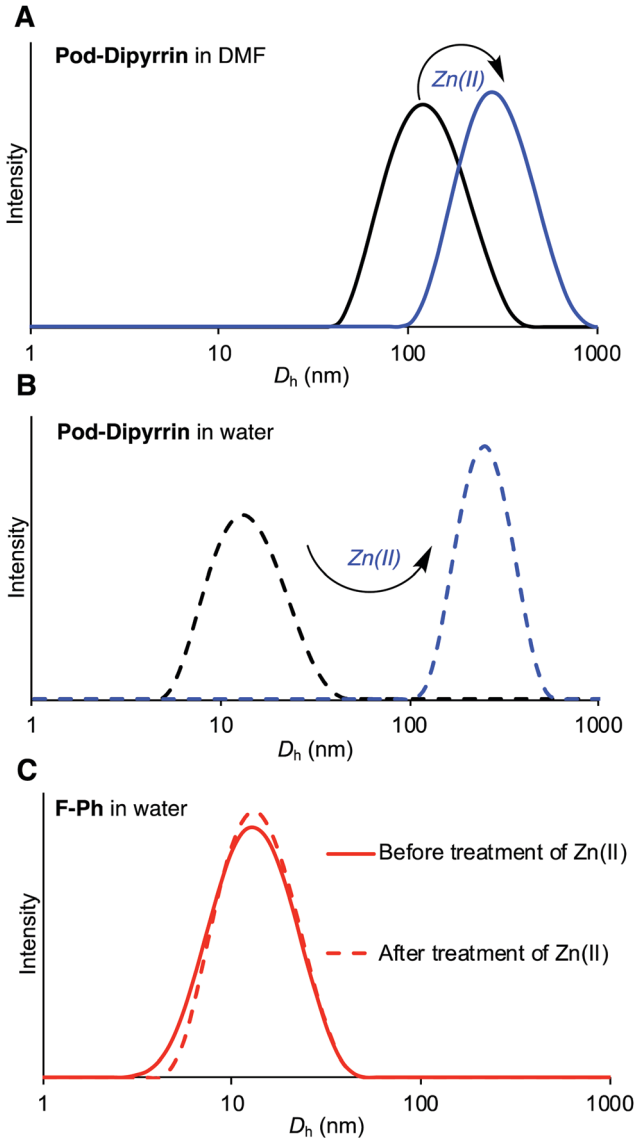

Fig. 8 DLS data at room temperature. (A) **Pod-Dipyrrin** in DMF before (black solid line) and after (blue solid line) treatment of Zn(II); (B) **Pod-Dipyrrin** in water before (black dashed line) and after (blue dashed line) treatment of Zn(II); (C) **F-Ph** in water before and after treatment with Zn(II). In all treatments, Zn(II) refers to $Zn(OAc)_2$ (440 equiv.).

1. Spectra and photophysics of dipyrrins

The chemistry of dipyrrins[25,26] is rapidly growing particularly because of the facile synthesis and versatile coordination features that can be exploited to create supramolecular structures.[27] The dipyrrinatoboron complexes (*i.e.*, BODIPYs)[28,29] are the best known but the bis(dipyrrinato)metal complexes have assembly features that the former lack. The fluorescence properties of dipyrrinato–metal complexes have been comprehensively reviewed,[11,27,30–32] including the turn-on fluorescence that accrues upon exposure of a free base dipyrrin to a suitable metal salt, termed chelation-enhanced fluorescence (CHEF).

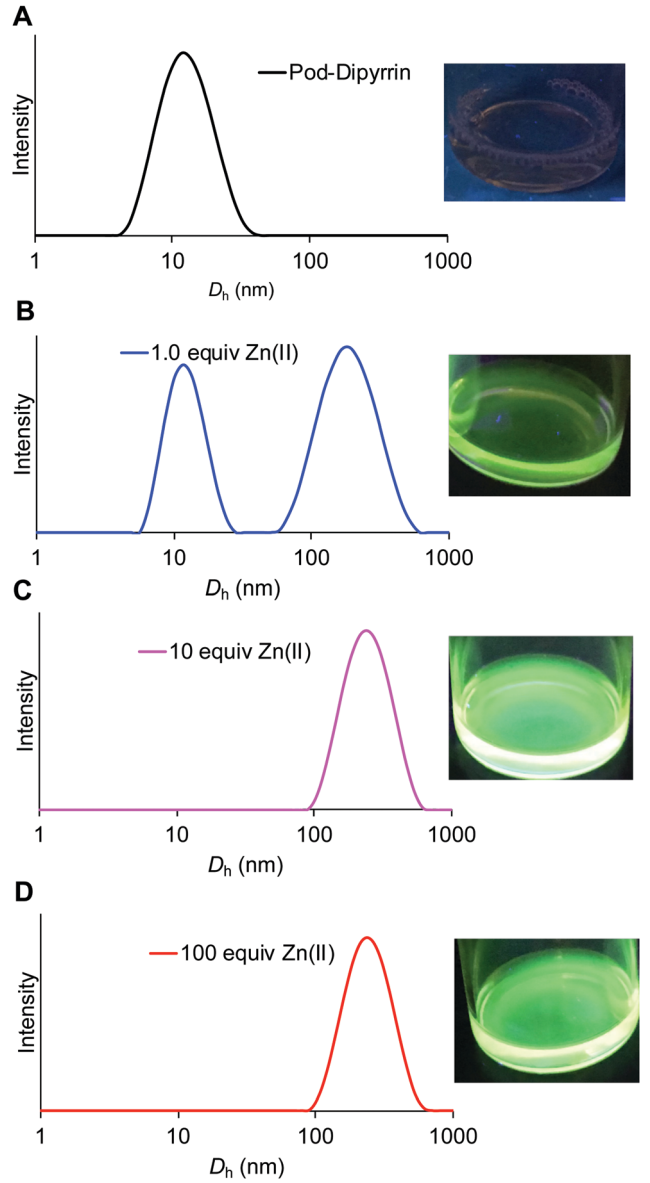

Fig. 9 All data were collected in water at room temperature. DLS data (left panel) and photographs of the **Pod-Dipyrrin** solution under ultraviolet illumination (right panel). (A) **Pod-Dipyrrin**; (B) **Pod-Dipyrrin** treated with 1.0 equivalent of Zn(II); (C) **Pod-Dipyrrin** treated with 10 equivalents of Zn(II); and (D) **Pod-Dipyrrin** treated with 100 equivalents of Zn(II). In all treatments, Zn(II) refers to $Zn(OAc)_2$.

Free base dipyrrins are at best only very weakly fluorescent,[30–32] although distinctions between one extreme of "complete lack of fluorescence"[33] and no fluorescence even at 1.2 K,[34] the common report of no detectable fluorescence ($\Phi_f < 5 \times 10^{-4}$;[35] ≤ 0.001;[11,32,36–38] $\leq 10^{-4}$;[39]), and the other extreme of a measurable albeit tiny fluorescence ($\Phi_f = 8.1 \times 10^{-4}$;[40] 2×10^{-3};[41] 0.01–0.02;[42]) may stem in part from different structural features of the dipyrrin in question. Some studies concerned the HBr salt of the free base dipyrrin, which may remain partially complexed in solution and contribute to the observed properties. Regardless, the photodynamics of free base dipyrrins were recognized early on to be dominated by internal conversion rather than by intersystem crossing.[34,41] Obvious mechanisms for internal conversion include rotation of the pyrrolic planes from coplanarity with respect to each other, and proton tunneling from the pyrrolic unit to the neighboring imino nitrogen.[34] A very recent study points instead, however, to the presence of a conical intersection of the S_1 and S_0 potential energy surfaces; such an intersection is less accessible energetically upon coordination of the nitrogen atoms. If the latter view holds, the diminished non-radiative decay upon metal coordination to the dipyrrin is less about structural rigidification and absence of proton transfer than shifting of molecular orbital energies.[43]

Here, three observations concerning the fluorescence of the **Pod-Dipyrrin** system warrant discussion. First, the **Pod-Dipyrrin** exhibits very low fluorescence in DMF (Φ_f = 0.0021) but ~1.7-fold increase upon foldamer assembly in water, albeit to a still very low value (Φ_f = 0.0035) (Fig. 1 and 3). The dipyrrin in the foldamer undergoes a striking spectral change in the unfolded state in DMF (broad, unstructured absorption) to the folded and compact unimer in water (more sharp absorption) (Fig. 4C). The origin of such spectral change is unclear, as the dipyrrin in the foldamer in aqueous solution (*versus* that in the extended conformation in DMF) is in a more hydrophobic environment, may be somewhat constrained conformationally, and perhaps is hydrogen-bonded where (1) the backbone N–H serves as the hydrogen-bond donor, (2) the amide carbonyl serves as a hydrogen-bond acceptor, and/or (3) the lone carboxylic acid at the polymer terminus serves as a proton donor. Such hydrogen bonds to and from the dipyrrin would likely supplant the known intramolecular hydrogen bond of the dipyrrin[44] and hence are only conjectural; a general rigidification of the dipyrrin owing to the constrained environment of the assembly may also contribute. Evidence for assembly of the compact unimer stems not only from the DLS data but also, *inter alia*, from 2D ^{1}H NMR NOESY analysis of polymer **F-Ph** in DMSO-d_6 or D_2O.[2] The Φ_f value of a cyanine dye also increased (by 2.5-fold) upon encapsulation in the pod architecture.[2]

Second, complexation with Zn(II) to form **(Pod-Dipyrrin)$_2$Zn(II)** causes the fluorescence intensity to be turned up markedly in DMF (Φ_f = 0.11) and for the compact unimer in water (Φ_f = 0.17) (Fig. 5B), resembling that of the dipyrrin lacking the attached foldamer (Fig. 1, Table 1); on the other hand, the already low fluorescence quantum yield of the free base dipyrrin is further *turned down* (to the level of noise) by complexation with Cu(II) to form **(Pod-Dipyrrin)$_2$Cu(II)** (Fig. 6A and B). The absorption spectral features of the **(Pod-Dipyrrin)$_2$Zn(II)** differ slightly in water *versus* DMF (compare Fig. 5A and 7); both the significant spectral changes of the dipyrrin and slight spectral changes of the bis(dipyrrinato)Zn(II) unit in DMF and water will require further investigation.

Third, treatment of **(Pod-Dipyrrin)$_2$M(II)**, where M = Cu or Zn, with EDTA in each case failed to give full reversion to the expected (limited) fluorescence of the free base dipyrrin (Fig. 5B and 6B). A tentative interpretation is that the M(II)–EDTA complex may associate with the **Pod-Dipyrrin** and cause quenching of the free base dipyrrin. Exploring the photophysics of the dipyrrins, particularly upon metal complexation,[45–49]

remains an area of active investigation, and gaining a deep understanding will require further experimental and theoretical work.

2. Polarity-dependent fluorescence probe in the self-assembled polymer

The fluorescence quantum yields of bis(dipyrrinato)Zn(II) complexes bearing α- and/or β-alkyl substituents are known to be dependent on solvent polarity.[50,51] Such complexes are fluorescent in a non-polar solvent such as toluene, but weakly or essentially non-fluorescent in modestly polar organic solvents (*e.g.*, dichloromethane). The diminution in fluorescence is attributed to an energetically accessible and non-emissive excited-state charge-transfer process.[50,51] The benchmark bis(dipyrrinato)Zn(II) complex **6** also exhibited a decrease in Φ_f value with increasing solvent polarity, but the effect was of lesser magnitude over a greater range of polarity: the decline was ~4.5-fold in total over the increase in polarity from toluene to DMF (Fig. 2 and Table 1). The benchmark bis(dipyrrinato)Zn(II) complex **6** lacks α- and β-alkyl substituents; alkyl substituents can profoundly alter the energetics of pyrrole molecules[52] and are similarly expected to influence the energetics of dipyrrin analogues.

The solvent-dependence of the fluorescence of bis(dipyrrinato)-Zn(II) complexes can be exploited as an initial gauge of the polarity of the "Pod". The Φ_f values of **(Pod-Dipyrrin)$_2$Zn(II)** in water (0.17) and DMF (0.11) compared with **6** in toluene (0.18) and DMF (0.041) indicate that in water (Tables 1 and 2), the bis(dipyrrinato)Zn(II) complex of **(Pod-Dipyrrin)$_2$Zn(II)** is in a nonpolar environment comparable to that of toluene. The hydrophobic environment is attributed to the pendant lauryl groups and the polymer backbone in the folded assembly. This agrees with our previously reported several ''Pod-fluorophores'', which have Φ_f values in aqueous solution similar to those of their hydrophobic benchmarks in toluene.[2] On the other hand, in DMF the bis(dipyrrinato)Zn(II) complex of **(Pod-Dipyrrin)$_2$Zn(II)** exhibits fluorescence intensity that reflects a modestly polar environment, but still less polar than that upon full exposure to bulk DMF. More in-depth analysis of the local environment will require examination of solvatochromic chromophores that exhibit changes in spectra alone or in conjunction with changes in fluorescence intensity.

3. Self-assembly and mechanical change

Self-assembly processes afford larger architectures the structures of which are manifested by the spontaneous interactions of the individual constituents.[53–58] While self-assembling architectures offer numerous attractive features, some limitations remained to be addressed. Common methods to characterize supramolecular assemblies include NMR spectroscopy, mass spectrometry, and microscopy (if size permits), all of which can pose difficulties in interpretation, which is rendered more complex when a distribution of species is present in an equilibrium mixture. Moreover, many self-assembly processes need to be carried out in organic solution given that most of the materials are hydrophobic, shutting off many applications in life sciences.

The **Pod-Dipyrrin** in aqueous solution is folded, compact and unimeric as evidenced by DLS interrogation (D_h = 15 nm) over a range of concentrations but is more extended in the organic solvent DMF (D_h = 140 nm) (Fig. 4A and B). In DMF, the dimeric **(Pod-Dipyrrin)$_2$Zn(II)** remains intact as evidenced by absorption and fluorescence spectroscopy (Fig. 7) yet exhibits a size approximately twice that of the monomer (D_h = 310 *versus* 140 nm). While we cannot rule out assemblies due to multimer aggregation, the cleanliness of the DLS data (Fig. 4A, B, 5C, 8 and 9) upon adding zinc acetate is consistent with (1) complete reaction of **F-Ph** with **5** to form the **Pod-Dipyrrin** construct (no signal corresponding to a monomer remained upon adding excess zinc acetate), and (2) a monomer – dimer system (no signals corresponding to intermediate or larger assemblies were observed). In DMF, both **Pod-Dipyrrin** and **(Pod-Dipyrrin)$_2$Zn(II)** architectures are expected to be extended with exploration of diverse conformational landscapes. On the other hand, in water, treatment with Zn(II) causes the folded, compact unimeric **Pod-Dipyrrin** to partially unfold upon metal-ion binding and join with another unfolded **Pod-Dipyrrin** to make a dimer. The change in size – from D_h = 15 nm to 260 nm indicates the unimer has largely unfolded. The **(Pod-Dipyrrin)$_2$Zn(II)** has rather similar size in DMF (D_h ~ 310 nm) and water (D_h ~ 260 nm) consistent with a largely extended conformation in both solvents, in contrast to the distinct sizes for the free base **Pod-Dipyrrin** (D_h = 140 nm *versus* 15 nm) in the same solvents in the absence of Zn(II) complexation.

Toward the end of this study we returned to examine a minor feature of the absorption spectrum of the **(Pod-Dipyrrin)$_2$Zn(II)**. The absorption spectrum shown in Fig. 5A exhibits a small shoulder (~517 nm) on the long-wavelength side of the main peak, which is not characteristic of typical bis(dipyrrinato)Zn(II) complexes as illustrated by **6** in diverse solvents (Fig. 1 and 2) and the **(Pod-Dipyrrin)$_2$Zn(II)** in DMF (Fig. 7). Illumination into the long-wavelength shoulder did not result in any distinguishable fluorescence apart from that of the **(Pod-Dipyrrin)$_2$Zn(II)**. Complexation of **Pod-Dipyrrin** with Zn(II) containing other counterions (chloride, triflate, sulfate) at 10 equiv. or 440 equiv. gave the **(Pod-Dipyrrin)$_2$Zn(II)** with a clean absorption spectrum lacking the long-wavelength shoulder and also the expected unimeric behavior as assessed by DLS spectroscopy (Fig. S1, see ESI†). The presence of the long-wavelength shoulder is tentatively attributed to the effect of the acetate counterion (although the molecular origin remains unknown) and does not alter the conclusions concerning assembly and disassembly of the fluorogenic bis(dipyrrinato)Zn(II) complex. During the course of these ZnX_2 complexation experiments, two observations were made concerning the size of the **(Pod-Dipyrrin)$_2$Zn(II)** complexes in water (Fig. S1 and S2, ESI†): (1) the size decreased by 9–30 nm in going from 10 to 440 equiv. of ZnX_2, and (2) the use of 440 *versus* 10 equiv. of $ZnCl_2$ or $Zn(OAc)_2$ resulted in slight broadening of the peak observed upon DLS examination. The change in size distribution may reflect specific effects of counterions as well as a general electrostriction, and warrants further examination.

The size of the assembled complex **(Pod-Dipyrrin)$_2$Zn(II)** in water or DMF is comparable to or larger than the discrete assemblies derived from metals and organic ligands bearing

two or three free base dipyrrin ligands.[59] In limited studies where the **Pod-Dipyrrin** was titrated with Zn(II), no intermediates were observed; in other words, the assembly to give the **(Pod-Dipyrrin)$_2$Zn(II)** was an all-or-nothing phenomena giving the homoleptic product. In contrast, a dibenzo-annulated 1,9-dicarboethoxydipyrrin (L–H) embedded in a dendrimer for aqueous solubilization underwent complexation with zinc acetate to give the heteroleptic complex MLX where M = Zn(II) and X = acetate; the architecture was proposed as a biosensor for detection of Zn(II).[60]

Outlook

In summary, the single-polymer–single cargo strategy with a dipyrrin as the cargo has revealed fundamental features concerning the conformational pliability of the amphiphilic polymer. The presence of a divalent ion (Zn(II), Cu(II)) triggers profound conformational change of the polymer–dipyrrin architecture. The molecular architecture of **Pod-Dipyrrin** may be unusual – and with fecund possibilities in supramolecular chemistry – in that mechanical change prompted by Zn(II) is accompanied by a striking ~50-fold increase in fluorescence. The change in fluorescence is visible by the naked eye although the change in absorption, while measurable by absorption spectroscopy, is far less evident by visual inspection. A common and versatile approach for metal ion sensing relies on binding to the lone pair of electrons on an amino group, thereby suppressing photoinduced electron transfer to an adjacent chromophore, thereby unleashing fluorescence.[61] The fluorogenic mechanism here, based on dipyrrin dimerization, is complementary. The bis(dipyrrinato)metal assembly process is robust and can be reversed by metal ion sequestration. Mechanosensory receptors, which sense mechanical changes caused by pressure, vibration or electric fields, are well known in biology.[62] Given the importance of mobile Zn(II) as a signaling molecule in neurophysiology,[63–65] the ability to chelate Zn(II), detect the chelation fluorogenically, and also exert a mechanical change may enable the design of novel sensory-mechanical constructs for fundamental manipulations in neurobiology.

Experimental procedures and characterization data

General methods

All chemicals obtained commercially were used as received unless otherwise noted. Reagent-grade solvents (CH_2Cl_2, hexanes, methanol, toluene, ethyl acetate) and HPLC-grade solvents (toluene, CH_2Cl_2, hexanes) were used as received. THF was freshly distilled from sodium/benzophenone ketyl and used immediately. Electrospray ionization mass spectrometry (ESI-MS) data are reported for the cationized molecular ion.

Synthesis

5-(4-Iodo-2,6-dimethylphenyl)dipyrromethane (2). Following an established procedure,[21,22] a solution of 4-iodo-2,6-dimethylbenzaldehyde (**1**,[12,13] 1.82 g, 7.00 mmol) in pyrrole (50.3 g, 52.0 mL, 750 mmol) was degassed with a stream of Ar for 20 min. Trifluoroacetic acid (82.0 mg, 54.0 μL, 700 μmol) was then added, and the solution was stirred under Ar at room temperature for 15 min. The solution was concentrated and chromatographed [silica, hexanes/CH_2Cl_2/ethyl acetate (75 : 20 : 5)] to obtain a pale yellow solid (1.58 g, 60% yield): mp 162–163 °C; ^{1}H NMR (400 MHz, $CDCl_3$) δ 2.06 (s, 6H), 5.90 (s, 1H), 5.96–5.98 (m, 2H), 6.17–6.20 (m, 2H), 6.68–6.70 (m, 2H), 7.43 (s, 2H), 7.95 (s, 2H); ^{13}C NMR (100 MHz, $CDCl_3$) δ 20.5, 38.7, 93.2, 107.1, 109.0, 116.8, 130.5, 137.8, 138.4, 140.3; ESI-MS obsd 377.0495, calcd 377.0509 [(M + H)$^+$, M = $C_{17}H_{17}IN_2$]; anal. calcd for $C_{17}H_{17}IN_2$: C, 54.27; H, 4.55; N, 7.45. Found: C, 54.09; H, 4.44; N, 7.27.

5-[4-(6-(*tert*-Butoxycarbonylamino)hexylaminocarbonyl)-2,6-dimethylphenyl]dipyrromethane (3). Following an established carbonylation procedure,[21,22] a Schlenk flask containing samples of **2** (188 mg, 500 μmol), $Pd(OAc)_2$ (11.0 mg, 50.0 μmol), Xantphos (29.0 mg, 50.0 μmol) and cesium carbonate (490 mg, 1.50 mmol) was evacuated and purged with carbon monoxide. A solution of *N*-(*tert*-butoxycarbonyl)-1,6-diaminohexane (216 mg, 1.00 mmol) in toluene (5.00 mL) was purged with Ar (30 min) and subsequently with carbon monoxide (30 min). The resulting solution was transferred into the Schlenk flask containing the solid materials under an atmosphere of CO. The reaction flask was placed in a preheated oil bath and stirred for 2 h at 90 °C. The resulting mixture was allowed to cool to room temperature. The solid material was filtered off and washed with toluene. The filtrate was concentrated, and the resulting residue was chromatographed [silica, hexanes/ethyl acetate (2 : 1)] to obtain a pale yellow solid (150 mg, 61% yield): mp 55–58 °C; ^{1}H NMR (300 MHz, $CDCl_3$) δ 1.35–1.52 (m, 13H), 1.56–1.66 (m, 4H), 2.13 (s, 6H), 3.11 (q, J = 6.6 Hz, 2H), 3.43 (q, J = 6.6 Hz, 2H), 4.54 (br s, 1H), 5.93–5.95 (m, 2H), 5.97 (s, 1H), 6.17 (q, J = 3.0 Hz, 2H), 6.29 (br s, 1H), 6.68 (dd, J_1 = 2.4 Hz, J_2 = 4.2 Hz, 2H), 7.43 (s, 2H), 7.98 (s, 2H); ^{13}C NMR (100 MHz, $CDCl_3$) δ 20.9, 26.1, 26.3, 28.5, 29.6, 30.1, 38.9, 39.7, 40.2, 79.2, 106.8, 108.6, 116.8, 128.0, 130.5, 133.1, 138.2, 141.5, 156.3, 167.6; ESI-MS obsd 515.2991, calcd 515.2993 [(M + Na)$^+$, M = $C_{29}H_{40}N_4O_3$]; λ_{abs} (CH_2Cl_2) 406 nm.

5-[4-(6-(*tert*-Butoxycarbonylamino)hexylaminocarbonyl)-2,6-dimethylphenyl]dipyrrin (4). Following an established procedure,[9] a solution of **3** (98.0 mg, 200 μmol) and *p*-chloranil (62.0 mg, 250 μmol) in THF (5.00 mL) was sonicated in a laboratory sonication bath for 1 h. The solution was concentrated and chromatographed [silica, hexanes/ethyl acetate (2 : 1)] to obtain a yellow solid (68.0 mg, 69% yield): mp 58–60 °C; ^{1}H NMR (400 MHz, $CDCl_3$) δ 1.36–1.55 (m, 15H), 1.66 (qt, J = 7.2 Hz, 2H), 2.18 (s, 6H), 3.16 (q, J = 6.4 Hz, 2H), 3.48 (q, J = 6.4 Hz, 2H) 4.58 (m, 1H), 6.32 (dq, J_1 = 1.2 Hz, J_2 = 4.8 Hz, 4H), 6.43 (br s, 1H), 7.53 (s, 2H), 7.63 (t, J = 1.2 Hz, 2H); ^{13}C NMR (100 MHz, $CDCl_3$) δ 20.2, 26.2, 26.4, 28.6, 29.7, 30.2, 39.8, 40.3, 79.2, 118.2, 125.8, 127.1, 134.6, 137.7, 139.6, 140.0, 144.0, 156.3, 167.8; ESI-MS obsd 491.3013, calcd 41.3017 [(M + H)$^+$, M = $C_{29}H_{38}N_4O_3$]; λ_{abs} (CH_2Cl_2) 429 nm.

5-[4-(6-(6-Maleimidohexanoylamino)hexylaminocarbonyl)-2,6-dimethylphenyl]dipyrrin (5). A solution of **4** (49.0 mg, 100 μmol) in CH_2Cl_2 (1.50 mL) was purged with Ar (for 5 min).

Trifluoroacetic acid (1.50 mL) was added, and the mixture was stirred for 12 h at room temperature. The volatile components (solvent and trifluoroacetic acid) were removed by purging with Ar. The resulting residue was treated with HBTU (76.0 mg, 200 μmol), 6-maleimidohexanoic acid (32.0 mg, 150 μmol), CH_2Cl_2 (5.00 mL) and *N,N*-diisopropylethylamine (500 μL) under Ar. The resulting solution was stirred for 2 h at room temperature. The mixture was concentrated and chromatographed [silica, ethyl acetate (2 : 1)] to obtain a brown solid (45.0 mg, 77% yield): mp 44–46 °C; ^{1}H NMR (300 MHz, $CDCl_3$) δ 1.26–1.69 (m, 14H), 2.15–2.20 (m, 8H), 3.26 (q, J = 6.6 Hz, 2H), 3.46–3.53 (m, 4H), 5.69 (m, 1H), 6.31–6.35 (m, 4H), 6.45 (br s, 1H), 6.68 (s, 2H), 7.52 (s, 2H), 7.63 (s, 2H); ^{13}C NMR (100 MHz, $CDCl_3$) δ 20.3, 25.4, 26.2, 26.3, 26.5, 28.5, 29.7, 29.8, 36.7, 37.8, 39.2, 39.8, 118.3, 125.8, 127.2, 134.3, 134.6, 137.7, 139.7, 140.0, 144.0, 167.9, 171.0, 173.0; ESI-MS obsd 584.3231, calcd 584.3231 [$(M + H)^+$, M = $C_{34}H_{41}N_5O_4$]; λ_{abs} (CH_2Cl_2) 468 nm.

Bis[5-(4-(6-(*tert*-butoxycarbonylamino)hexylaminocarbonyl)-2,6-dimethylphenyl)dipyrrinato]zinc(II) (6). A solution of **4** (15 mg, 30 μmol) in $CHCl_3$ (2.0 mL) was treated with $Zn(OAc)_2{\cdot}2H_2O$ (33 mg, 150 μmol, 10 equiv.) in methanol (0.5 mL). After stirring for 15 h at room temperature, the mixture was diluted with $CHCl_3$, washed with water, dried with anhydrous sodium sulfate and chromatographed [silica, hexanes/ethyl acetate, (1 : 1)]. Decomplexation occurred during chromatography, and the starting material **4** was recovered. The reaction was repeated in identical fashion with the recovered material. The mixture was washed with water. The organic layer was concentrated to dryness to obtain a red solid (13.6 mg, 85% yield): mp 205 °C (discoloration); ^{1}H NMR (400 MHz, $CDCl_3$) δ 1.40–1.54 (m, 30H), 1.68 (qt, J = 6.8 Hz, 4H), 2.27 (s, 12H), 3.16 (q, J = 6.4 Hz, 4H), 3.50 (q, J = 6.4 Hz, 4H), 4.58 (br s, 2H), 6.37 (d, J = 4.4 Hz, 4H), 6.43 (br t, J = 4.8 Hz, 2H), 6.52 (d, J = 4 Hz, 4H), 7.49 (br s, 4H), 7.57 (br s, 4H); ^{13}C NMR (100 MHz, $CDCl_3$) δ 20.3, 26.2, 26.4, 28.7, 29.9, 30.3, 39.9, 40.4, 79.3, 117.8, 125.7, 131.1, 134.5, 137.6, 139.5, 141.5, 146.9, 149.8, 156.4, 167.9; ESI-MS obsd 1043.5079, calcd 1043.5096 [$(M + H)^+$, M = $C_{58}H_{74}N_8O_6Zn$]; λ_{abs} (toluene) 487 nm, ε_{488nm} = 52 900 M^{-1} cm^{-1}.

Pod-Dipyrrin

A solution of **F-Ph**[2] (30 mg), **5** (0.53 mg, 0.90 μmol), and ethanolamine (0.24 μL) in DMF (400 μL) was treated with triethylamine (1 drop). The resulting mixture was stirred at room temperature for 16 h. Then the mixture was diluted with 1.0 mL of DMF. The resulting solution was transferred into a dialysis membrane as described in a prior ESI†[2] in detail. The solution was then dialyzed in DMF to remove the excess fluorophore. The dialysis reservoir volume was replaced with fresh DMF four times over the course of ~24 h. The resulting solution was dried under high vacuum at 50 °C, and the resulting solid was dissolved in DI water. The aqueous solution was then freeze-dried to give a pink solid (26 mg). The characterization and properties of the construct are described in the Results section.

Absorption spectroscopy

Absorption spectra were recorded at room temperature as described previously.[2] Unless stated otherwise, samples were examined with **Pod-Dipyrrin** at ~20 μM (A ~ 1 in a 1 cm pathlength cuvette).

Fluorescence spectroscopy

Fluorescence spectra were recorded as described previously[2] at room temperature using **BDPY-hydrazide** in methanol (Φ_f = 0.97)[2,24] and **II** in toluene (Φ_f = 0.36)[10] as quantitative standards with correction for instrument sensitivity but without correction for solvent refractive indices. Unless stated otherwise, samples were examined with **Pod-Dipyrrin** at ~2 μM in a 1 cm pathlength cuvette. The typical wavelength of excitation of the **(Pod-Dipyrrin)$_2$Zn(II)** was into the short-wavelength shoulder at ~460 nm.

Dynamic light scattering (DLS) measurements

DLS analysis of the **Pod-Dipyrrin** was performed in cuvettes with a Zetasizer Nano ZS instrument. A typical analysis was as follows: a sample was dissolved in HPLC-grade water containing 1.0 M NaCl (filtered with a 220 nm membrane) for analysis, in some cases with a preceding step of filtration through a 220 nm membrane. Illumination was performed at 632.8 nm at room temperature. Unless stated otherwise, samples were examined with **Pod-Dipyrrin** at ~20 μM.

Nuclear magnetic resonance (NMR) spectroscopy

^{1}H NMR spectra were measured at room temperature.

Metal coordination reactions

The number of equivalents of a metal salt in a coordination reaction of a dipyrrin is described relative to the bis(dipyrrinato)-metal complex; *e.g.*, 5.5 μmol of $Zn(OAc)_2$ and 0.025 μmol of **Pod-Dipyrrin** corresponds to 440 equiv. of $Zn(OAc)_2$.

General method for metal coordination reactions of Pod-Dipyrrin, illustrated with Zn(II) in water

A solution of **Pod-Dipyrrin** in water (1.0 mg mL^{-1}) was measured directly, without dilution, by DLS and absorption spectroscopy in a 1 cm pathlength cuvette. Then a part of the solution (~200 μL) was diluted (by ~6-fold) by water and transferred into another 1 cm pathlength cuvette. The resulting solution measured by absorption and fluorescence spectroscopy. A solution of **Pod-Dipyrrin** (1.0 mL, 1.0 mg mL^{-1}) was treated with $Zn(OAc)_2$ (1.0 mg, 5.5 μmol, ~440 equivalent of **Pod-Dipyrrin**). The resulting solution was allowed to sit for 5 min and measured directly, without dilution, by DLS and absorption spectroscopy in a 1 cm pathlength cuvette. Then a part of the Zn(II)-containing **Pod-Dipyrrin** solution (~200 μL) was diluted (by ~6-fold) by water and transferred into another 1 cm pathlength cuvette. The resulting solution was measured by absorption and fluorescence spectroscopy. The Zn(II) containing **Pod-Dipyrrin** solution (0.8 mL, 1.0 mg mL^{-1}) was treated with EDTA (4.0 mg, 14 μmol, ~3.2 equivalent per total Zn(II)). The resulting solution was allowed to sit for 5 min and measured directly, without dilution, by DLS and absorption spectroscopy in a 1 cm pathlength cuvette. Then a part of the EDTA treated **Pod-Dipyrrin** solution (~200 μL) was diluted

(by ~6-fold) by water and transferred into another 1 cm pathlength cuvette. The resulting solution was measured by absorption and fluorescence spectroscopy.

Metal binding reactions of Pod-Dipyrrin with Cu(II) in water

Following the method describe for the reaction of **Pod-Dipyrrin** with Zn(II), a solution of **Pod-Dipyrrin** in water (1.0 mL, 1.0 mg mL^{-1}) was treated with $CuCl_2$ (1.0 mg, 7.5 μmol, ~600 equivalent). The resulting solution was measured by DLS, absorption and fluorescence spectroscopy. Then the resulting solution was treated with EDTA (4.0 mg, 14 μmol, 2.3 equivalent per total Cu(II)) and measured by DLS, absorption and fluorescence spectroscopy.

Metal binding reactions of F-Ph with Zn(II) in water

Following the method describe for the reaction of **Pod-Dipyrrin** with Zn(II) in water, a solution of **F-Ph** in water (1.0 mL, 1.0 mg mL^{-1}) was measured by DLS spectroscopy and treated with $Zn(OAc)_2$ (1.0 mg, 5.5 μmol). The resulting solution was then measured by DLS spectroscopy.

Metal binding reactions of Pod-Dipyrrin with Zn(II) in DMF

Following the method describe for the reaction of **Pod-Dipyrrin** with Zn(II) in water, a solution of **Pod-Dipyrrin** in DMF (1.0 mL, 1.0 mg mL^{-1}) was measured by DLS, absorption and fluorescence spectroscopy. Then the mixture was treated with $Zn(OAc)_2$ (1.0 mg, 5.5 μmol, ~440 equivalent). The resulting solution was measured by DLS, absorption and fluorescence spectroscopy.

Conflicts of interest

J. S. L. is cofounder of NIRvana Sciences, which develops fluorophores for use in clinical diagnostics.

Acknowledgements

The synthesis of compounds **2–6** was supported in 2011–2013 by the Photosynthetic Antenna Research Center (PARC), an Energy Frontier Research Center funded by the U.S. Department of Energy, Office of Science, Office of Basic Energy Sciences, under Award No. DE-SC0001035. Extension of **5** to form the **Pod-Dipyrrin** for fundamental studies was supported by a grant (1R41GM131501) to NIRvana Sciences from the NIGMS. Mass spectrometry measurements were carried out in the Molecular Education, Technology, and Research Innovation Center (METRIC) at NC State University.

References

1 R. W. Wagner and J. S. Lindsey, *Pure Appl. Chem.*, 1996, **68**, 1373–1380. Corrigendum: R. W. Wagner and J. S. Lindsey, *Pure Appl. Chem.*, 1998, **70**(8), i.
2 R. Liu and J. S. Lindsey, *ACS Macro Lett.*, 2019, **8**, 79–83; R. Liu and J. S. Lindsey, *ACS Macro Lett.*, 2019, **8**, 154.
3 M. Kamigaito, T. Ando and M. Sawamoto, *Chem. Rev.*, 2001, **101**, 3689–3745.
4 M. Matsumoto, T. Terashima, K. Matsumoto, M. Takenaka and M. Sawamoto, *J. Am. Chem. Soc.*, 2017, **139**, 7164–7167.
5 Y. Bai, H. Xing, G. A. Vincil, J. Lee, E. J. Henderson, Y. Lu, N. G. Lemcoff and S. C. Zimmerman, *Chem. Sci.*, 2014, **5**, 2862–2868.
6 Y. Li, Y. Bai, N. Zheng, Y. Liu, G. A. Vincil, B. J. Pedretti, J. Cheng and S. C. Zimmerman, *Chem. Commun.*, 2016, **52**, 3781–3784.
7 M. Taniguchi, G. Hu, R. Liu, H. Du and J. S. Lindsey, Proc. S.P.I.E. BiOS, Reporters, Markers, Dyes, Nanoparticles, and Molecular Probes for Biomedical Applications X, 2018, vol. 10508, p. 1050806.
8 H. Fischer and M. Schubert, *Ber. Dtsch. Chem. Ges.*, 1924, **57**, 610–617.
9 L. Yu, K. Muthukumaran, I. V. Sazanovich, C. Kirmaier, E. Hindin, J. R. Diers, P. D. Boyle, D. F. Bocian, D. Holten and J. S. Lindsey, *Inorg. Chem.*, 2003, **42**, 6629–6647.
10 I. V. Sazanovich, C. Kirmaier, E. Hindin, L. Yu, D. F. Bocian, J. S. Lindsey and D. Holten, *J. Am. Chem. Soc.*, 2004, **126**, 2664–2665.
11 E. V. Antina, R. T. Kuznetsova, L. A. Antina, G. B. Guseva, N. A. Dudina, A. I. V'yugin and A. V. Solomonov, *Dyes Pigm.*, 2015, **113**, 664–674.
12 S. Kajigaeshi, T. Kakinami, H. Yamasaki, S. Fujisaki and T. Okamoto, *Bull. Chem. Soc. Jpn.*, 1988, **61**, 600–602.
13 R. W. Wagner, T. E. Johnson and J. S. Lindsey, *J. Am. Chem. Soc.*, 1996, **118**, 11166–11180.
14 B. J. Littler, M. A. Miller, C.-H. Hung, R. W. Wagner, D. F. O'Shea, P. D. Boyle and J. S. Lindsey, *J. Org. Chem.*, 1999, **64**, 1391–1396.
15 J. K. Laha, S. Dhanalekshmi, M. Taniguchi, A. Ambroise and J. S. Lindsey, *Org. Process Res. Dev.*, 2003, **7**, 799–812.
16 N.-F. K. Kaiser, A. Hallberg and M. Larhed, *J. Comb. Chem.*, 2002, **4**, 109–111.
17 J. Georgsson, A. Hallberg and M. Larhed, *J. Comb. Chem.*, 2003, **5**, 350–352.
18 X. Wu, R. Rönn, T. Gossas and M. Larhed, *J. Org. Chem.*, 2005, **70**, 3094–3098.
19 O. Lagerlund and M. Larhed, *J. Comb. Chem.*, 2006, **8**, 4–6.
20 B. Roberts, D. Liptrot, L. Alcaraz, T. Luker and M. J. Stocks, *Org. Lett.*, 2010, **12**, 4280–4283.
21 C. Ruzié, M. Krayer, T. Balasubramanian and J. S. Lindsey, *J. Org. Chem.*, 2008, **73**, 5806–5820.
22 J. R. Martinelli, D. A. Watson, D. M. M. Freckmann, T. E. Barder and S. L. Buchwald, *J. Org. Chem.*, 2008, **73**, 7102–7107.
23 H. L. Kee, C. Kirmaier, L. Yu, P. Thamyongkit, W. J. Youngblood, M. E. Calder, L. Ramos, B. C. Noll, D. F. Bocian, W. R. Scheidt, R. R. Birge, J. S. Lindsey and D. Holten, *J. Phys. Chem. B*, 2005, **109**, 20433–20443.
24 https://www.lumiprobe.com/p/bodipy-fl-hydrazide, accession date 09/10/2018.
25 T. E. Wood and A. Thompson, *Chem. Rev.*, 2007, **107**, 1831–1861.

26 T. E. Wood, I. Uddin and A. Thompson, in *Handbook of Porphyrin Science*, ed. K. M. Kadish, K. M. Smith and R. Guilard, World Scientific, Singapore, 2010, vol. 8, pp. 235–291.
27 R. Sakamoto, T. Iwashima, M. Tsuchiya, R. Toyoda, R. Matsuoka, J. F. Kögel, S. Kusaka, K. Hoshiko, T. Yagi, T. Nagayama and H. Nishihara, *J. Mater. Chem. A*, 2015, **3**, 15357–15371.
28 A. Treibs and F.-H. Kreuzer, *Liebigs Ann. Chem.*, 1968, **718**, 208–223.
29 A. Loudet and K. Burgess, *Chem. Rev.*, 2007, **107**, 4891–4932.
30 S. A. Baudron, *Dalton Trans.*, 2013, **42**, 7498–7509.
31 Y. Ding, Y. Tang, W. Zhu and Y. Xie, *Chem. Soc. Rev.*, 2015, **44**, 1101–1112.
32 E. V. Antina, N. A. Bumagina, A. I. V'yugin and A. V. Solomonov, *Dyes Pigm.*, 2017, **136**, 368–381.
33 T. M. McLean, D. Cleland, K. C. Gordon, S. G. Telfer and M. R. Waterland, *J. Raman Spectrosc.*, 2011, **42**, 2154–2164.
34 J. A. Pardoen, J. Lugtenburg and G. W. Canters, *J. Phys. Chem.*, 1985, **89**, 4272–4277.
35 H. Falk and F. Neufingerl, *Monatsh. Chem.*, 1979, **110**, 987–1001.
36 N. A. Dudina, E. V. Antina, G. B. Guseva, A. I. V'yugin and A. S. Semeikin, *Russ. J. Org. Chem.*, 2013, **49**, 1734–1739.
37 N. A. Dudina, E. V. Antina, G. B. Guseva and A. I. Vyugin, *J. Fluoresc.*, 2014, **24**, 13–17.
38 N. A. Dudina, E. V. Antina, D. I. Sozonov and A. I. V'yugin, *Russ. J. Org. Chem.*, 2015, **51**, 1155–1161.
39 D. Prasannan and C. Arunkumar, *New J. Chem.*, 2017, **41**, 11190–11200.
40 Y. Mei, C. J. Frederickson, L. J. Giblin, J. H. Weiss, Y. Medvedeva and P. A. Bentley, *Chem. Commun.*, 2011, **47**, 7107–7109.
41 V. A. Ganzha, G. P. Gurinovich, B. M. Dzhagarov, A. M. Shul'ga and A. N. Nizamov, *J. Appl. Spectrosc.*, 1987, **47**, 722–725.
42 M. A. Filatov, A. Y. Lebedev, S. N. Mukhin, S. A. Vinogradov and A. V. Cheprakov, *J. Am. Chem. Soc.*, 2010, **132**, 9552–9554.
43 M. Buyuktemiz, S. Duman and Y. Dede, *J. Phys. Chem. A*, 2013, **117**, 1665–1669.
44 S. A. Baudron, D. Salazar-Mendoza and M. W. Hosseini, *CrystEngComm*, 2009, **11**, 1245–1254.
45 C. Trinh, K. Kirlikovali, S. Das, M. E. Ener, H. B. Gray, P. Djurovich, S. E. Bradforth and M. E. Thompson, *J. Phys. Chem. C*, 2014, **118**, 21834–21845.
46 Y. S. Marfin and E. V. Rumyantsev, *Spectrochim. Acta, Part A*, 2014, **130**, 423–428.
47 A. A. Ksenofontov, G. B. Guseva and E. V. Antina, *Mol. Phys.*, 2016, **114**, 2838–2847.
48 A. A. Ksenofontov, G. B. Guseva, E. V. Antina and A. I. Vyugin, *J. Lumin.*, 2016, **170**, 275–281.
49 M. Tsuchiya, R. Sakamoto, M. Shimada, Y. Yamanoi, Y. Hattori, K. Sugimoto, E. Nishibori and H. Nishihara, *Inorg. Chem.*, 2016, **55**, 5732–5734.
50 S. Kusaka, R. Sakamoto, Y. Kitagawa, M. Okumura and H. Nishihara, *Chem. – Asian J.*, 2012, **7**, 907–910.
51 M. Asaoka, Y. Kitagawa, R. Teramoto, K. Miyagi, Y. Natori, R. Sakamoto, H. Nishihara and M. Nakano, *Polyhedron*, 2017, **136**, 113–116.
52 T. A. Nigst, M. Westermaier, A. R. Ofial and H. Mayr, *Eur. J. Org. Chem.*, 2008, 2369–2374.
53 J. S. Lindsey, *New J. Chem.*, 1991, **15**, 153–180.
54 G. M. Whitesides, E. E. Simanek, J. P. Mathias, C. T. Seto, D. N. Chin, M. Mammen and D. M. Gordon, *Acc. Chem. Res.*, 1995, **28**, 37–44.
55 D. S. Lawrence, T. Jiang and M. Levett, *Chem. Rev.*, 1995, **95**, 2229–2260.
56 P. J. Stang and B. Olenyuk, *Acc. Chem. Res.*, 1997, **30**, 502–518.
57 M. M. Conn and J. Rebek, Jr., *Chem. Rev.*, 1997, **97**, 1647–1668.
58 S. I. Stupp, V. LeBonheur, K. Walker, L. S. Li, K. E. Huggins, M. Keser and A. Amstutz, *Science*, 1997, **276**, 384–389.
59 S. A. Baudron, *CrystEngComm*, 2016, **18**, 4671–4680.
60 S. Thyagarajan, B. Ghosh, M. A. Filatov, A. V. Moore, A. V. Cheprakov and S. A. Vinogradov, *Proc. SPIE*, 2011, **7910**, 79100Z.
61 A. P. de Silva, T. S. Moody and G. D. Wright, *Analyst*, 2009, **134**, 2385–2393.
62 K. L. Marshall and E. A. Lumpkin, *Adv. Exp. Med. Biol.*, 2012, **739**, 142–155.
63 E. M. Nolan and S. J. Lippard, *Acc. Chem. Res.*, 2009, **42**, 193–203.
64 E. Tomat and S. J. Lippard, *Curr. Opin. Chem. Biol.*, 2010, **14**, 225–230.
65 R. J. Radford and S. J. Lippard, *Curr. Opin. Chem. Biol.*, 2013, **17**, 129–136.

